BIOCHEMISTRY
including biophysical chemistry & molecular biology

Article

pubs.acs.org/biochemistry

Pro-Oxidant Copper-Binding Mode of the Apo Form of ALS-Linked SOD1 Mutant H43R Denatured at Physiological Temperature

Nobuhiro Fujimaki, Furi Kitamura, and Hideo Takeuchi*

Graduate School of Pharmaceutical Sciences, Tohoku University, Aobayama, Sendai 980-8578, Japan

Supporting Information

ABSTRACT: The mutation of Cu,Zn-superoxide dismutase (SOD1), a major antioxidant enzyme, is associated with amyotrophic lateral sclerosis (ALS). In a previous study, we showed that the metal-depleted apo form of an ALS-linked mutant, H43R, undergoes denaturation at physiological temperature (37 °C) in 90 min and acquires pro-oxidant activity in the presence of Cu^{2+} and H_2O_2. In this study, we have examined the Cu^{2+}-binding mode of denatured apo-H43R by circular dichroism (CD), fluorescent oxidation, UV Raman spectroscopy, and photooxidation. CD spectroscopy indicates that denatured apo-H43R loses native β-barrel structure and the binding of Cu^{2+} to the denatured apo form induces local refolding. Fluorescent-oxidation assays in the absence and presence of Cu^{2+} chelators show that denatured apo-H43R contains two Cu^{2+}-binding sites with higher and lower Cu^{2+} affinities and with pro-oxidant activities in the reverse order. UV Raman spectroscopy gives evidence that His residues are bound to Cu^{2+} mainly through the imidazole Nτ atom at the higher-affinity site and through the Nπ atom at the lower-affinity site, sharing one His residue with each other. The Cu^{2+}-binding mode of denatured apo-H43R is analogous to but different from the Cu,Zn-binding mode of the native holo form. Photooxidation experiments confirm the involvement of His residues in the pro-oxidant activity. Taken together, it is suggested that the binding of Cu^{2+} induces the local refolding of denatured apo-H43R to create toxic catalytic centers that convert the enzyme from antioxidant to pro-oxidant, leading to the pathogenesis of ALS. His residues are essential for both Cu^{2+}-binding and pro-oxidant activities.

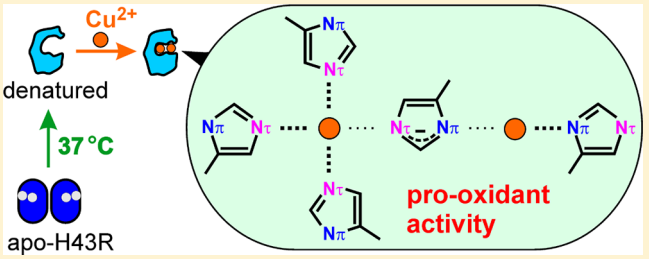

A variety of gene mutations of the cytosolic enzyme Cu,Zn-superoxide dismutase (SOD1) are associated with amyotrophic lateral sclerosis (ALS),[1−4] which is a fatal neurodegenerative disease characterized by a progressive loss of motor neurons in the brain and spinal cord.[5] Native SOD1 protects cells by catalyzing the dismutation of superoxide into less toxic hydrogen peroxide and molecular oxygen.[6] The pathogenesis of ALS was once supposed to be associated with a reduction of antioxidant activity in the SOD1 mutant. However, transgenic mice that express human SOD1 mutants with full dismutase activity also showed hallmarks of ALS pathology.[7,8] Accordingly, it is now considered that the ALS-linked mutant of SOD1 gains new cytotoxic properties responsible for the pathogenesis of ALS.[4,7,8] The new toxic properties proposed thus far include structural instability leading to the formation of cytotoxic self-aggregates[9−12] and pro-oxidant activity leading to an increase of cellular oxidative stress.[13−17]

Human SOD1 is a homodimer of a 153-amino acid subunit, which is folded into a β-barrel structure and contains one Cu^{2+} and one Zn^{2+}.[18] Wild-type SOD1 is very stable in structure and extremely efficient in its enzymatic activity.[19,20] In a previous study, we examined structural and enzymatic properties of an ALS-linked mutant of human SOD1, His43 → Arg (H43R).[21] Although the properties of the H43R mutant did not differ from those of the wild-type in the Cu,Zn-bound holo form, a striking difference was found between the mutant and wild-type in the metal-depleted apo form. The apo-H43R mutant gained a strong propensity to unfold or misfold into an irregular structure, whereas the wild-type apo form retained structural stability. The denaturation of apo-H43R to an unfolded structure occurred with a half-life of about 30 min under physiological conditions (37 °C, pH 7.4). Concomitant with the denaturation, apo-H43R acquired pro-oxidant potential, which was fully expressed in the presence of Cu^{2+} and H_2O_2. The acquisition of structural instability and pro-oxidant potential by apo-H43R implied a toxic role for the denatured apo forms of SOD1 mutants in the development of ALS.

The pro-oxidant activity of denatured apo-H43R in the presence of Cu^{2+} may be closely related to the binding mode of Cu^{2+}. Visible/near-infrared absorption spectra monitoring the Cu^{2+} d−d electronic transition showed that the denatured apo protein binds Cu^{2+} in a mode that is different from that in the native holo form,[21] although details of the Cu^{2+}-binding mode remained unclear. In this study, we have investigated the Cu^{2+}-binding mode of denatured apo-H43R by circular dichroism (CD), fluorescent oxidation, UV resonance Raman spectroscopy, and photooxidation. The results show that denatured

Received: March 22, 2013
Revised: June 20, 2013
Published: July 10, 2013

apo-H43R contains two Cu^{2+}-binding sites with different Cu^{2+} affinities and pro-oxidant activities. These binding sites are created by a local refolding of the denatured protein in the presence of Cu^{2+} and are composed of different numbers of His residues with different Cu^{2+}-coordination types. His residues are involved in the pro-oxidant activity as well. The Cu^{2+}-binding mode of denatured apo-H43R revealed here may be useful for understanding the cytotoxic properties of denatured, mismetalated SOD1 mutants in terms of its molecular structure.

MATERIALS AND METHODS

Preparation of Recombinant Human SOD1. Recombinant human SOD1 and its H43R and H43R/W32F mutants were prepared as described previously with slight modifications.[21] Briefly, the protein was expressed in *Escherichia coli* cells harboring plasmid pET15b, which contains a human SOD1 cDNA fused with an N-terminal hexa-His-tag. A QuikChange site-directed mutagenesis kit (Stratagene) was used to create the mutant genes. The plasmid-transformed *E. coli* cells were cultured in Luria−Bertani medium, harvested by centrifugation, and lysed in 20 mM Tris buffer (pH 7.5) supplemented with 20 mM imidazole, 1 mM β-mercaptoethanol (β-ME), 8 M urea, 1% (v/v) Triton, and 1% (w/v) streptomycin (Nacalai Tesque). After 1 h of stirring, the cell lysate was centrifuged to precipitate the insoluble material. His-tagged SOD1 was isolated from the supernatant by immobilized metal-ion affinity chromatography (IMAC) using a Ni^{2+}-charged medium (Ni Sepharose 6 Fast Flow, GE Healthcare) in a batch mode. The obtained His-tagged protein was first dialyzed against 10 mM Tris-HCl (pH 7.4) containing 0.5 mM β-ME to remove urea and then against 10 mM Tris-HCl (pH 7.4) supplemented with 100 μM $(CH_3COO)_2Zn$, 0.1 M NaCl, and 0.5 mM β-ME to refold the protein. After the removal of excess Zn^{2+} with 0.1 mM ethylenediaminetetraacetic acid (EDTA), the His tag was cleaved from the refolded protein with thrombin (GE Healthcare). Further purification of the His-tag-removed protein was performed on Ni^{2+}-charged IMAC (HisTrap HP, GE Healthcare) and gel-filtration columns (Sephacryl-100, GE Healthcare). The purified protein was lyophilized and stored at −80 °C.

Preparation of Denatured Apo-H43R and Apo-H43R/W32F. The apo form of the H43R or H43R/W32F mutant was prepared from the purified protein by a 48 h dialysis against 50 mM sodium acetate (pH 3.8) containing 10 mM EDTA.[21] The removal of EDTA and subsequent buffer exchange were performed by two successive 24 h dialyses against 50 mM sodium acetate (pH 3.8) and 50 mM sodium phosphate (pH 7.4), respectively. The protein concentration (in monomer units) was determined using the bicinchoninic acid (BCA) assay that is based on the alkaline reduction of Cu^{2+} to Cu^{+} by protein.[21] Bovine SOD1 (Calzyme Laboratories), with a molar extinction coefficient of 10 300 M^{-1} cm^{-1} at 258 nm in the dimeric holo form,[6] was used as a standard protein to calibrate the absorption intensity at 562 nm of the BCA−Cu^{+} complex. The denatured forms of apo-H43R and apo-H43R/W32F were prepared by incubating the protein solution at 37 °C for 90 min as described previously.[21]

Assay for the Pro-Oxidant Activity of Denatured Apo-H43R. The pro-oxidant activity of apo-H43R was assayed using the oxidation of nonfluorescent 2′,7′-dichlorodihydrofluorescein (DCFH) to fluorescent 2′,7′-dichlorofluorescein (DCF) as described previously.[21] The oxidation of DCFH was initiated by mixing DCFH (50 μM), H_2O_2 (50 μM), and denatured apo-H43R (10 μM in monomer units) in 50 mM phosphate buffer (pH 7.4) with or without the addition of Cu^{2+} ($CuCl_2$, 0−60 μM). The solution was kept in the dark for 5 min at room temperature and immediately subjected to fluorescence analysis (excitation at 495 nm and emission at 524 nm). The fluorescence assay based on the oxidation of DCFH to DCF (hereafter called DCF fluorescence assay) was also performed in the presence of a metal chelator, nitrilotriacetic acid (NTA) or EDTA, to investigate the effect of Cu^{2+} depletion on the pro-oxidant activity of denatured apo-H43R.

Assay for the Number of Cu^{2+} Ions Bound to Denatured Apo-H43R. The quantitative determination of Cu^{2+} in Cu^{2+}-bound denatured apo-H43R was performed colorimetrically by using 4-(2-pyridylazo)resorcinol (PAR), which exhibits a large increase in absorption at 500 nm upon binding to Cu^{2+}.[23] Denatured apo-H43R was first mixed with 1 or 2.5 equiv of Cu^{2+} in 50 mM phosphate buffer (pH 7.4), and the solution was dialyzed against Cu^{2+}-free phosphate buffer overnight to remove unbound Cu^{2+}. The remaining Cu^{2+}-bound protein was divided into two samples of equal volume. One sample was subjected to a BCA assay to determine the protein concentration.[22] The other sample was incubated at 37 °C for 5 min in borate buffer (100 mM, pH 7.8) containing 6 M guanidine-HCl (denaturant) and 100 μM PAR.[24] The concentration of Cu^{2+} in the protein solution was determined from the absorbance at 500 nm using a calibration line obtained with standard Cu^{2+} solutions (Wako). The number of Cu^{2+} ions per monomer unit of denatured apo-H43R was calculated from the ratio of the Cu^{2+} and protein concentrations.

Photooxidation of Denatured Apo-H43R. To gain information on the amino acid residues involved in the pro-oxidant activity, denatured apo-H43R was photooxidized. The protein was mixed with rose bengal (RB), a sensitizer of photooxidation,[25,26] in 50 mM phosphate buffer (pH 7.4). The concentrations of the protein and sensitizer were 20 and 1.5 μM, respectively. The solution was then irradiated with a fluorescent lamp (27 W) for 1, 3, or 5 min. The photooxidation was monitored as an increase in the absorbance at 250 nm.[27]

Preparation of Model Compounds Containing His−Cu^{2+} Bonds. (Glycyl-L-histidinato)copper(II) (GlyHis−Cu^{2+}), in which His is bound to Cu^{2+} through the imidazole Nπ atom (HisNπ−Cu), was prepared by mixing 2.8 mM aqueous $CuCl_2$ with an equivalent volume of 2.8 mM glycyl-L-histidine dissolved in 10 mM aqueous NaOH.[28] The solution was lyophilized, and the solid product was dissolved in D_2O at a concentration of 1.4 mM. The pD was adjusted to 6 with DCl. Separately, β-alanyl-L-histidine was mixed with Cu^{2+} to prepare the homodimer of (β-alanyl-L-histidinato)copper(II) (β-Ala-His−Cu^{2+}) in which His is bound to Cu^{2+} through the imidazole Nτ atom (HisNτ−Cu).[29] The solution was lyophilized, and the solid product was dissolved in D_2O at a concentration of 1.4 mM and pD 10.5. Glycylglycine (GlyGly) forms a chelation compound with Cu^{2+} (GlyGly−Cu^{2+}) that further binds to deprotonated imidazole (imidazolate, Im^{-}) at a 2:1 molar ratio to form an imidazolate-bridged binuclear complex, $(GlyGly-Cu^{2+})_2-Im^{-}$.[30] We mixed GlyGly−$Cu^{2+}$ with L-His instead of imidazole to prepare an analogous compound, $(GlyGly-Cu^{2+})_2-His^{-}$, in which deprotonated His was expected to bridge two Cu^{2+} ions ($His^{-}-Cu_2$). The replacement of imidazole by L-His was necessary because the vibrations of imidazole significantly differ from those of His, and the imidazole complex is not suited for the analysis of

dx.doi.org/10.1021/bi400370w | *Biochemistry* 2013, 52, 5184−5194

Raman spectra of proteins.[31] Briefly, GlyGly−Cu^{2+} (16 mM) was prepared by dissolving equimolar GlyGly and $CuCl_2$ in H_2O at pH 7.0. Then, the GlyGly−Cu^{2+} solution was mixed with 10 mM L-histidine at a Cu^{2+}/His molar ratio of 2:1. The pH of the solution was adjusted to 10.7 with NaOH to stabilize the binuclear complex.[30] After lyophilization, the complex was dissolved in D_2O at a concentration of 1.4 mM. The pD of the final solution was adjusted to 10.7 by adding NaOD.

UV Raman Spectra. Protein samples for UV Raman spectral measurements were prepared as follows. The denatured apo proteins (H43R and H43R/W32F) were dissolved in 5 mM phosphate buffer (pH 7.4) at a concentration of 40 μM. Next, an equivalent volume of $CuCl_2$ solution (40 or 100 μM) or phosphate buffer (for Cu^{2+}-free samples) was added to the solution. After lyophilization to remove H_2O, the dried sample was dissolved in D_2O at a protein concentration of 200 μM. The solvent exchange from H_2O to D_2O was conducted to observe better the Raman bands of the metal-coordinated imidazole ring of His.[32−38] The Raman spectra of GlyHis−Cu^{2+}, β-AlaHis−Cu^{2+}, and $(GlyGly-Cu^{2+})_2$−His^- were also recorded in D_2O solution (1.4 mM). The Raman band of D_2O at 1210 cm^{-1} was used as an internal intensity standard both for the proteins and His model compounds.

UV Raman spectra were excited at 229 nm using continuous-wave radiation from an intracavity frequency-doubled Ar^+ ion laser (Coherent Innova 300 FReD) and recorded on a UV Raman spectrometer (Jasco TR-600UV) equipped with a liquid-nitrogen-cooled CCD detector (Princeton Instruments LN/CCD-1752). The sample solution was spun in a spinning quartz cell, and the laser power was 1 to 2 mW at the sample. Typically, Raman spectra were recorded with an accumulation time of 6−10 min, and the spectra recorded for three to eight fresh samples were averaged. The Raman spectrum of a cyclohexanone−acetonitrile mixture (1:1, v/v) was used for wavenumber calibration. The decomposition of overlapping Raman bands was performed by assuming a Voigt profile (a convolution of Gaussian and Lorentzian profiles) for the individual component bands.[39,40] A laboratory-made software, RaspWin, was used for the band decomposition.

Fluorescence, CD, and Absorption Spectra. Fluorescence spectra were recorded on a Jasco FP-6300DS spectrofluorometer using a 3 × 3 mm^2 quartz cell. A Jasco J-820 spectropolarimeter was used for measuring CD spectra in a quartz cell with a 0.5 mm path length. UV−vis absorption spectra were recorded in a quartz cell with a 5 mm path length using a Hitachi U-3300 spectrophotometer.

RESULTS

Effect of Cu^{2+} Binding on the Secondary Structure. Denatured apo-H43R acquires pro-oxidant activity when bound to Cu^{2+}, as reported previously.[21] As a first step to elucidate the Cu^{2+}-binding mode of denatured apo-H43R, we examined the effect of Cu^{2+} addition on the secondary structure of the protein by CD spectroscopy. Figure 1 shows CD spectra of denatured apo-H43R (prepared by incubation at 37 °C for 90 min) in the absence and presence of Cu^{2+}. The spectra of native apo-H43R (before incubation at 37 °C) and native holo-H43R are also shown for comparison. In the absence of Cu^{2+}, denatured apo-H43R exhibits a negative band at 199 nm because of its irregular structure.[41] With an increase in the Cu^{2+} concentration, the negative peak becomes weaker, suggesting that the binding of Cu^{2+} induces a partial refolding of the protein. (Hereafter, we will use the term "Cu^{2+}-bound denatured apo-H43R" to mean the apo-H43R protein that was denatured by incubation at 37 °C for 90 min and metalated by the addition of Cu^{2+} ions.) The spectrum of fully Cu^{2+}-bound denatured apo-H43R (in the presence of 3 equiv of Cu^{2+}) is clearly different from those of native apo-H43R and native holo-H43R. In particular, the negative intensity around 210 nm is characteristic of a β-sheet,[21,41] an essential element of the native β-barrel structure, which is significantly weaker than those of the native apo and holo forms. This observation suggests that the β-barrel structure of the native form is destroyed to some extent in denatured apo-H43R and the Cu^{2+} binding induces a local refolding of the denatured protein without recovering the β-barrel structure.

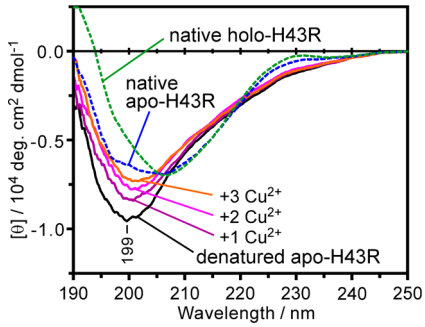

Figure 1. CD spectra of denatured apo-H43R (incubated at 37 °C for 90 min) in the absence and presence (1, 2, and 3 equiv) of Cu^{2+}. The spectra of native apo-H43R (before incubation at 37 °C) and native holo-H43R are also shown for comparison. The protein was dissolved in phosphate buffer (50 mM, pH 7.4) at a concentration of 20 μM. Cu^{2+} was added as $CuCl_2$.

Number of Cu^{2+}-Binding Sites in Denatured Apo-H43R. The pro-oxidant activity of denatured apo-H43R in the presence of varied amounts of Cu^{2+} was measured by DCF fluorescence assay, which is a sensitive method for detecting reactive oxygen species.[42] Analogous DCF fluorescence assays were also performed for native apo-H43R. The intensity of the fluorescence from DCF, produced by the oxidation of DCFH, is plotted against the molar ratio of Cu^{2+} to apo-H43R (monomer unit) in Figure 2. The fluorescence intensity is very

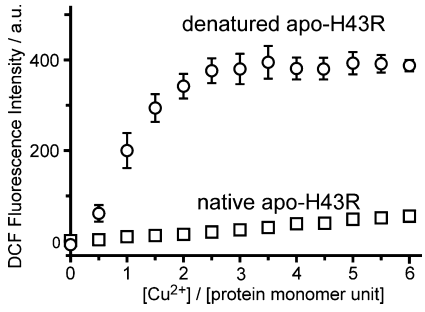

Figure 2. Pro-oxidant activity of native and denatured apo-H43R as a function of the Cu^{2+}/protein molar ratio. The pro-oxidant activity was measured as the fluorescence intensity from DCF produced by the oxidation of DCFH (50 μM) in the presence of denatured apo-H43R (10 μM), $CuCl_2$ (0−60 μM), and H_2O_2 (50 μM). The DCF fluorescence was excited at 495 nm and observed at 523 nm. Error bars represent the standard errors of the mean (n = 3). For native apo-H43R, no repeated measurements were made because the fluorescence intensity was close to the background level observed for the protein-free control samples.

dx.doi.org/10.1021/bi400370w | Biochemistry 2013, 52, 5184−5194

small for native apo-H43R throughout a 0−6 range of the Cu^{2+}/protein ratio. (The Cu^{2+} ion induces similarly weak DCF fluorescence even in the absence of protein.) For denatured apo-H43R, however, the fluorescence intensity steeply increases with an increase of the Cu^{2+}/protein ratio from 0 to 2, reaching a plateau at about 2.5. The saturation of the fluorescence intensity is not due to the lack of reactants because the addition of horseradish peroxidase, a pro-oxidant enzyme, further induced green fluorescence of DCF. Figure 2 gives evidence that the pro-oxidant activity is unique to the denatured form, and it reaches a maximum in the presence of 2.5 equiv of Cu^{2+}. The saturation of the pro-oxidant activity at 2.5 equiv of Cu^{2+} indicates that the number of Cu^{2+}-binding sites in denatured apo-H43R is not greater than 2.5. Our previous CD spectroscopic study revealed that the denaturation of apo-H43R takes place as a two-state transition from the native to the denatured form, with each having a well-defined secondary structure.[21] Accordingly, the denatured form of apo-H43R is unique in secondary structure and contains an integer number of Cu^{2+}-binding sites that is less than 2.5 (i.e., one or two).

To determine precisely the number of Cu^{2+}-binding sites in denatured apo-H43R, we measured the molar ratio of Cu^{2+} and protein in the Cu^{2+}-bound protein using the PAR and BCA colorimetric assays, respectively. Denatured apo-H43R was mixed with 1 or 2.5 equiv of Cu^{2+} and dialyzed to remove unbound Cu^{2+} followed by PAR and BCA assays. The molar ratio of Cu^{2+} to the protein monomer unit was 1.02 ± 0.07 (n = 5) when 1 equiv of Cu^{2+} was mixed with the protein, and the Cu^{2+}/protein ratio was raised to 1.90 ± 0.15 (n = 7) when 2.5 equiv of Cu^{2+} was added to the protein solution. These results give evidence that denatured apo-H43R has two Cu^{2+}-binding sites per monomer unit.

Cu^{2+} Affinities and Pro-Oxidant Activities of the Cu^{2+}-Binding Sites. The examination of the Cu^{2+} affinities and pro-oxidant activities of the two Cu^{2+}-binding sites were performed by a DCF fluorescence assay in the presence of metal-chelating agents. The chelators used are NTA and EDTA, whose Cu^{2+}-complex formation constants (log K) are 12.9 and 18.8, respectively.[43] Control DCF fluorescence assays showed no pro-oxidant activity for Cu^{2+}-bound NTA and EDTA. First, a given amount of NTA (a moderate chelator) was added to a solution of denatured apo-H43R (10 μM) saturated with 2.5 equiv of Cu^{2+}, and the pro-oxidant activity of the protein was measured by DCF fluorescence assay. Figure 3A shows the dependence of the observed DCF fluorescence intensity on the NTA concentration. With an increase in the NTA concentration, the fluorescence intensity decreases exponentially, reaching a plateau at about 3 mM NTA. The addition of EDTA (a strong chelator) at this point further reduces the fluorescence intensity exponentially toward a background level. These observations clearly indicate that the two Cu^{2+}-binding sites have significantly different affinities for Cu^{2+}: the site with a higher affinity releases Cu^{2+} only in the presence of the strong chelator EDTA (hereafter called the higher-affinity site), whereas the other site with a lower affinity is demetalated even by the weak chelator NTA (lower-affinity site). The plot in Figure 3A also suggests a difference in the pro-oxidant activity between the two Cu^{2+}-binding sites. The lower-affinity site is likely to have a higher pro-oxidant activity than the higher-affinity site because the reduction of pro-oxidant activity (DCF fluorescence intensity) by NTA is about twice that by EDTA (Figure 3A).

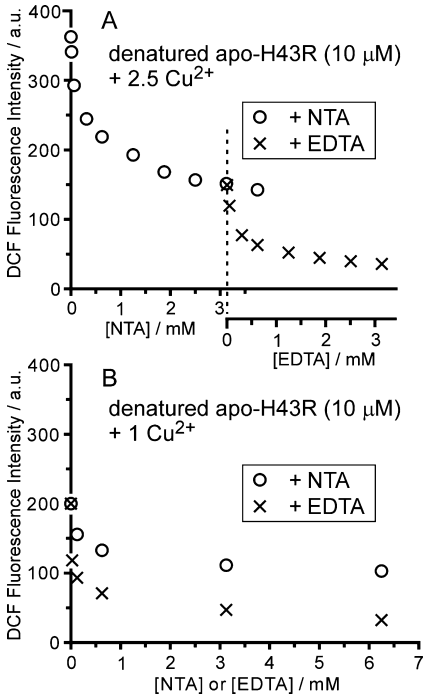

Figure 3. Effect of Cu^{2+} depletion on the pro-oxidant activity of Cu^{2+}-bound denatured apo-H43R. The pro-oxidant activity was measured as the fluorescence intensity from DCF produced by the oxidation of DCFH (50 μM) in the presence of denatured apo-H43R (10 μM), $CuCl_2$ (10 μM), H_2O_2 (50 μM), and one or two chelators (NTA and/or EDTA, 0−6.2 mM). The DCF fluorescence was excited at 495 nm and observed at 523 nm. NTA was added first and then EDTA was added in panel A, whereas NTA or EDTA was added separately in panel B.

Denatured apo-H43R mixed with only 1 equiv of Cu^{2+} was also treated with NTA and EDTA followed by the DCF fluorescence assay. Figure 3B shows the effects of the chelators on the DCF fluorescence intensity. NTA reduces the fluorescence intensity to about 50% at maximum, whereas EDTA almost eliminates the fluorescence. These observations are consistent with the Cu^{2+} affinities and pro-oxidant activities of the higher- and lower-affinity sites. In the presence of 1 equiv of Cu^{2+}, the higher-affinity site may be more populated with Cu^{2+} than the lower-affinity site. Although NTA removes Cu^{2+} ions from only the less-populated lower-affinity site, this site possesses higher pro-oxidant activity as described above. Therefore, it is not unreasonable that the removal of Cu^{2+} from the lower-affinity site by NTA causes about a 50% reduction in the pro-oxidant activity, as seen in Figure 3B. However, EDTA removes the Cu^{2+} ions from both sites, resulting in a nearly complete loss of the activity. The chelation experiments with NTA and EDTA confirm that there are two Cu^{2+}-binding sites; one site with a higher Cu^{2+} affinity and lower pro-oxidant activity (higher-affinity site) and the other site with a lower Cu^{2+} affinity and higher pro-oxidant activity (lower-affinity site).

Raman Spectroscopic Examination of the Cu^{2+}-Bound Amino Acid Residues. Raman spectroscopy is a powerful tool for studying protein structures including metal-binding modes.[32−38] In particular, excitation with UV light has the advantage that the Raman scattering is resonance-enhanced for UV-absorbing components such as aromatic amino acid residues and main-chain amides,[44−46] some of which are

dx.doi.org/10.1021/bi400370w | Biochemistry 2013, 52, 5184−5194

expected to serve as ligands for metal cations. In this study, we have applied UV-resonance Raman spectroscopy to the examination of the Cu^{2+}-binding mode of denatured apo-H43R. Figure 4 compares the 229 nm-excited Raman spectra of

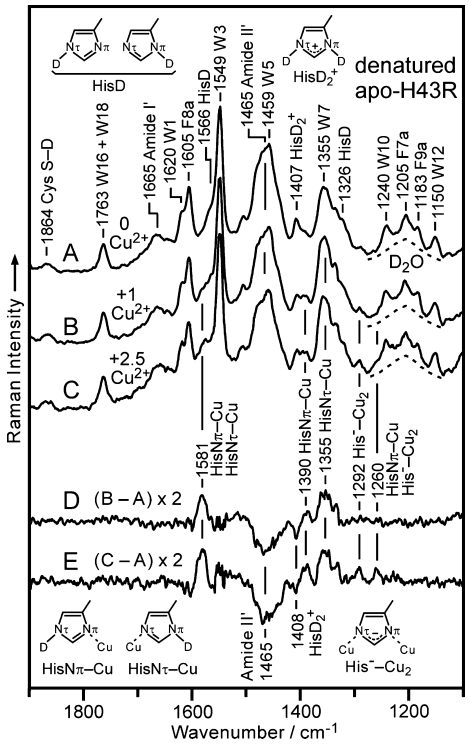

Figure 4. UV (229 nm) Raman spectra of denatured apo-H43R (200 μM) (A) and its mixture with 1 (B) and 2.5 (C) equiv of Cu^{2+} dissolved in D_2O phosphate buffer. The pD values were 7.4, 7.4, and 7.0 for A, B, and C, respectively. The difference spectra B minus A (D) and C minus A (E) are also shown. The 1210 cm^{-1} D_2O band was used as an internal intensity standard in the computation of the difference spectra. The insets show the structures of N-deuterated neutral (HisD), cationic ($HisD_2^+$), and Cu^{2+}-bound forms (HisNπ–Cu, HisNτ–Cu, and His^-–Cu_2) of the His imidazole ring.

D_2O solutions of denatured apo-H43R in the absence and presence of Cu^{2+}. The D_2O solution was employed to observe even weak Raman bands of His.[32−38]

In the absence of Cu^{2+}, the Raman spectrum is composed of many bands (Figure 4A), most of which are assigned to Phe (the bands denoted with F7a, F8a, and F9a), Trp (W1, W3, W5, W7, W10, W12, and W16 + W18), and main-chain amides (Amide I′ and Amide II′).[44−47] Weak shoulder bands resulting from N-deuterated neutral His (HisD) and cationic His ($HisD_2^+$) are also seen.[32,36,37] Additionally, a weak band observed at 1864 cm^{-1} is ascribed to the S–D stretch of Cys.[48] In the presence of 1 or 2.5 equiv of Cu^{2+}, small spectral changes appear at several wavenumber positions (Figure 4B,C). To examine the effects of Cu^{2+} addition on the Raman spectrum, we computed difference spectra by subtracting the spectrum in the absence of Cu^{2+} (Figure 4A) from that in the presence of Cu^{2+} (Figure 4B or 4C). A broad band around 1210 cm^{-1} resulting from D_2O was used as an internal intensity standard in the computation of the difference spectra.

Figure 4D,E shows the 4B minus 4A and 4C minus 4A difference spectra expanded by a factor of 2, respectively. Compared to the original spectra, the difference spectra are simple and the Raman bands due to Phe, Trp, and Cys are absent in the difference spectra. It is possible that the negative band around 1465 cm^{-1} and the positive band at 1355 cm^{-1} are contributed from the W5 (1459 cm^{-1}) and W7 (1355 cm^{-1}) bands of Trp. However, the lack of Trp contribution to the difference spectra was confirmed by the observation that a Trp-deficient mutant (H43R/W32F) mixed with 1 equiv of Cu^{2+} gave a difference spectrum very similar to Figure 4D (Supporting Information, Figure S1). The absence of the Phe, Trp, and Cys Raman bands in the difference spectra indicates that four Phe, one Trp, and two free-Cys residues contained in each monomer unit are not involved in the Cu^{2+} binding. The sharp negative peak at 1408 cm^{-1} in Figure 4D,E is assigned to $HisD_2^+$, which was converted to a metal-bound form in the presence of Cu^{2+}. Another board negative band around 1465 cm^{-1} is ascribed to a change in the amide II′ vibration. The possibility of Cu^{2+} coordination to deprotonated main-chain amide groups is excluded because no Raman band characteristic of a deprotonated amide is seen around 1430 cm^{-1}.[34,49] The intensity decrease of the Amide II′ band may reflect a change in secondary structure upon binding of Cu^{2+}, as revealed by CD spectroscopy (Figure 1).

The imidazole ring of His has two nitrogen atoms (Nπ and Nτ) that can serve as ligands to Cu^{2+}. Therefore, three types of Cu^{2+}-bound His are possible: either Nπ or Nτ is used to bind a Cu^{2+} ion (HisNπ–Cu or HisNτ–Cu) or both Nπ and Nτ are used to bind different Cu^{2+} ions (His^-–Cu_2). H43R contains seven His residues per monomer unit, and the positive bands at 1581, 1390, 1355, 1292, and 1260 cm^{-1} in Figure 4D,E are assigned to HisNπ–Cu/HisNτ–Cu, HisNπ–Cu, HisNτ–Cu, His^-–Cu_2, and HisNπ–Cu/His^-–Cu_2, respectively, as indicated in the figure.[36,37] The bands resulting from His^-–Cu_2 are negligibly weak in the presence of 1 equiv of Cu^{2+} but are evident in the presence of 2.5 equiv of Cu^{2+}, suggesting that two Cu^{2+}-binding sites can share a His residue, which forms an imidazolate bridge when both Cu^{2+}-binding sites are filled with Cu^{2+}.

UV Raman Spectra of His Model Compounds. As a basis for evaluating the number of Cu^{2+}-bound His from the intensities of Raman bands in Figure 4, we measured the Raman spectra of model compounds containing HisNπ–Cu, HisNτ–Cu, and His^-–Cu_2. Figure 5A–C shows the Raman spectra of GlyHis, β-AlaHis, and a 2:1 mixture of GlyGly and His in the absence and presence of Cu^{2+}. In the absence of Cu^{2+} (lower trace in each panel of Figure 5), most Raman bands are ascribed to His.[37] Among them, the band at 1373 to 1374 cm^{-1} completely disappears in the presence of Cu^{2+} (upper trace), indicating the absence of Cu^{2+}-free His. It is also noted that Cu^{2+}-bound His generally gives sharper and stronger Raman bands than the Cu^{2+}-free His. GlyHis forms a Cu^{2+} complex containing HisNπ–Cu (Figure 5A),[28] whereas β-AlaHis forms another Cu^{2+} complex containing HisNτ–Cu (Figure 5B).[29] Most Raman bands in Figure 5A,B are assigned to the expected forms of His–Cu^{2+} coordination[36,37] or to the Cu^{2+}-bound deprotonated amide ($Amide^-$–Cu), as indicated in the figure.[34,49] For the mixture of GlyGly, His, and Cu^{2+} (Figure 5C, upper trace), we expected the formation of (GlyGly–Cu^{2+})$_2$–His^- containing one His^-–Cu_2 imidazolate bridge. However, the Raman spectrum (upper trace) exhibits a few bands that are assigned to HisNπ–Cu in addition to the 1289 cm^{-1} band arising from His^-–Cu_2.[36,37] This observation indicates that the imidazolate bridge is partially broken at the Nτ site in (GlyGly–Cu^{2+})$_2$–His^-.

dx.doi.org/10.1021/bi400370w | Biochemistry 2013, 52, 5184−5194

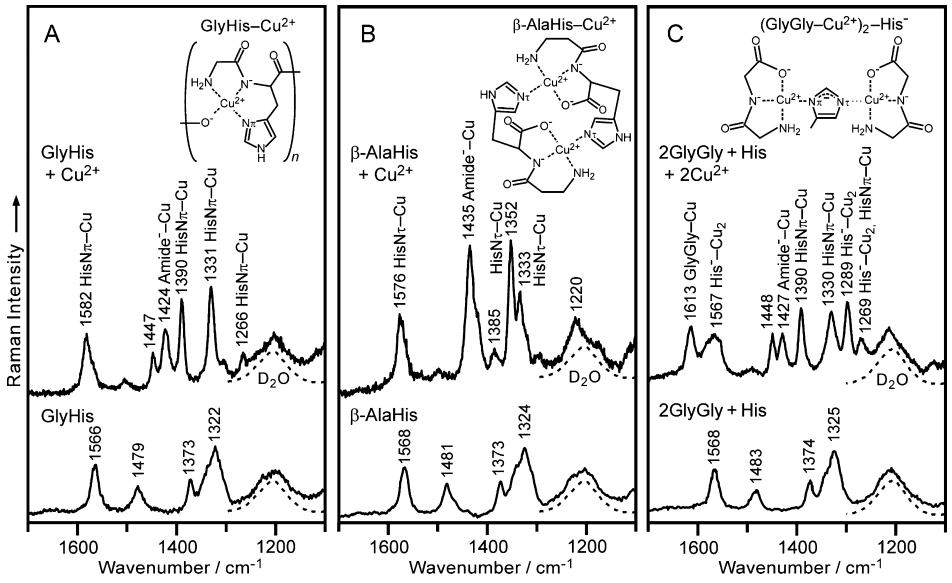

Figure 5. UV (229 nm) Raman spectra of GlyHis (A), *β*-AlaHis (B), and a 2:1 mixture of GlyGly and His in the absence (lower trace) and presence (upper trace) of Cu^{2+} (C). The His model compounds were dissolved in D_2O at a concentration of 1.4 mM. The pD values were 6, 10.5, and 10.7 for A, B, and C, respectively. The insets in A and B show the structures of the corresponding Cu^{2+} complexes in the crystalline state.[28,29] The structure in C is drawn in an analogous matter to that of the crystal structure of a complex of imidazole with 2 mols of GlyGly–Cu^{2+}.[30] The replacement of imidazole by His seems to break the imidazolate bridge at the Nτ atom to some extent because the Raman bands characteristic of HisNπ–Cu are observed at 1390 and 1330 cm^{-1}.

Evaluation of the Numbers of Cu^{2+}-Bound His Residues in Three Different Coordination Types. To evaluate quantitatively the numbers of HisNπ–Cu, HisNτ–Cu, and His^-–Cu_2 in Cu^{2+}-bound denatured apo-H43R from the Raman difference spectra in Figure 4D,E, we computed analogous difference spectra for the three His model compounds in Figure 5. The difference spectra of apo-H43R and the model compounds were decomposed into component bands by assuming Voigt band shapes.[39] Figure 6 compares the results of band decomposition in the 1410–1270 cm^{-1} region where the marker bands of HisNπ–Cu, HisNτ–Cu, and His^-–Cu_2 are seen at ~1390, ~1355, and ~1295 cm^{-1}, respectively. The integrated intensities of the bands resulting from HisNπ–Cu, HisNτ–Cu, and His^-–Cu_2 in Figure 6 were measured relative to the 1210 cm^{-1} band of D_2O in the original spectra and converted to the values per molar of apo-H43R or His for the model compounds. The Raman intensities thus obtained are listed in Table 1. GlyHis–Cu^{2+} contains one HisNπ–Cu, and its Raman intensity serves as a standard for evaluating the number of HisNπ–Cu in Cu^{2+}-bound denatured apo-H43R. Similarly, the Raman intensity of the HisNτ–Cu band of *β*-AlaHis–Cu^{2+} can be used for evaluating the number of HisNτ–Cu. In $(GlyGly–Cu^{2+})_2–His^-$, HisNπ–Cu and His^-–Cu_2 coexist, as revealed by Figure 5C. By comparing the intensity of the HisNπ–Cu Raman band between GlyHis–Cu^{2+} and $(GlyGly–Cu^{2+})_2–His^-$, the imidazolate bridge is estimated to be broken at the Nτ site for 70% of $(GlyGly–Cu^{2+})_2–His^-$. Thus, the remaining complex (30%) retains the imidazolate bridge, and its Raman intensity may be used to evaluate the number of His^-–Cu_2 in denatured apo-H43R. The values in parentheses in Table 1 indicate the number of HisNπ–Cu, HisNτ–Cu, and His^-–Cu_2 calculated from the Raman intensity. In the presence of 1 equiv of Cu^{2+}, denatured apo-H43R contains 0.5 HisNπ–Cu and 2.8 HisNτ–Cu, whereas 1.1 HisNπ–Cu, 3.1 HisNτ–Cu, and 0.3 His^-–Cu_2 are formed in the presence of 2.5 equiv of Cu^{2+}.

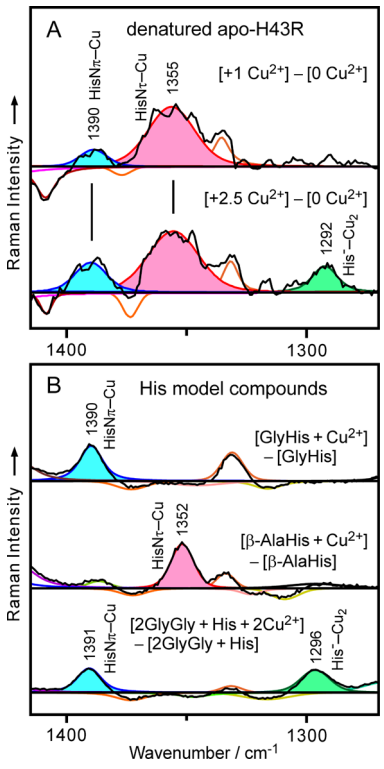

Figure 6. Comparison of Raman difference spectra of Cu^{2+}-bound denatured apo-H43R (A) (derived from the spectra in Figure 4) and Cu^{2+} complexes of His model compounds (B) (derived from the spectra in Figure 5). The Raman intensity was calibrated with the D_2O band at 1210 cm^{-1} in the original spectra. The integrated intensities of the difference signals were evaluated after decomposition of the spectrum into component bands with Voigt shapes. Three key bands resulting from HisNπ–Cu, HisNτ–Cu, and His^-–Cu are filled with different colors.

dx.doi.org/10.1021/bi400370w | *Biochemistry* 2013, 52, 5184–5194

Table 1. Observed Raman Band Intensities and the Corresponding Numbers of Cu^{2+}-Bound His Residues in Three Different Coordination Types[a]

compound	HisNπ–Cu (1390 cm^{-1})[b]	HisNτ–Cu (1355 cm^{-1})[b]	His^{-}–Cu_2 (1292 cm^{-1})[b]
denatured apo-H43R + 1 Cu^{2+}	187 (0.5)	1119 (2.8)	
denatured apo-H43R + 2.5 Cu^{2+}	408 (1.1)	1229 (3.1)	303 (0.3)
GlyHis–Cu^{2+}	381 (1)[c]		
β-AlaHis–Cu^{2+}		403 (1)[c]	
$(GlyGly–Cu^{2+})_2$–His^{-}[c]	273 (0.7)[d]		272 (0.3)[c,d]

[a]The integrated intensities were measured relative to the 1210 cm^{-1} D_2O band and converted to the values per molar of the protein or His for the model compounds. The number of His residues obtained from the Raman intensity is given in parentheses. [b]Wavenumbers observed for Cu^{2+}-bound denatured apo-H43R. [c]Intensity standard used for calculating the number of Cu^{2+}-bound His residues. [d]The imidazolate bridge (His^{-}–Cu_2) is broken at the Nτ site for 70% of the complex as judged from the intensity of the HisNπ–Cu Raman band. The remaining complex (30%) retains the imidazolate bridge.

Effect of Photooxidation of His on the Pro-Oxidant Activity. The Raman spectral data presented above have shown that Cu^{2+} is bound to His residues of denatured apo-H43R. To check the possible involvement of His residues in the pro-oxidant activity of Cu^{2+}-bound denatured apo-H43R, we photooxidized the denatured protein with RB and measured the pro-oxidant activity in the presence of 1 equiv of Cu^{2+} by DCF fluorescence assay. His is known to be most vulnerable to RB-sensitized photooxidation among the amino acids composing proteins.[25−27] Figure 7 shows the effect of photooxidation on the UV absorption spectrum and the DCF fluorescence intensity. With an increase in the duration of photoirradiation, the absorbance at 250 nm increases (Figure 7A), indicating the oxidation of His residues.[27,50] No significant change is seen for the Trp absorption band around 280 nm. Concomitant with the oxidation of His, the DCF fluorescence intensity decreases, and about 50% of the fluorescence intensity is lost in 5 min of photoirradiation (Figure 7B). This observation clearly shows that one or more His residues are involved in the pro-oxidant activity of Cu^{2+}-bound denatured apo-H43R.

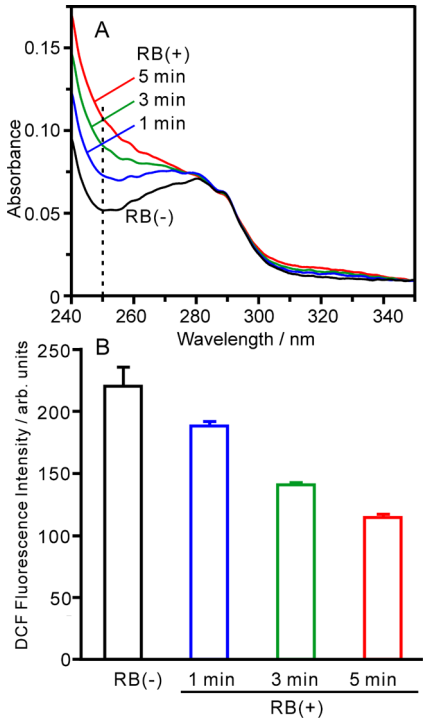

Figure 7. Effects of photooxidation with RB on the absorption spectrum (A) and the pro-oxidant activity (B) of denatured apo-H43R. Denatured apo-H43R (20 μM) was mixed with RB (1.5 μM) in 50 mM phosphate buffer (pH 7.4) and irradiated with a fluorescent lamp (27 W) for 1, 3, or 5 min. After photoirradiation, the absorption spectrum of the sample was recorded. The pro-oxidant activity of the photoirradiated protein was measured by DCF fluorescence assay as described in the legend for Figure 2. The error bars in B represent the standard errors of the mean (n = 3). The absorption spectrum and pro-oxidant activity before photooxidation are also shown as RB(−) for comparison.

DISCUSSION

Cu^{2+}-Binding Mode of Denatured Apo-H43R. The present DCF fluorescence assays in the absence and presence of Cu^{2+} chelators have shown that denatured apo-H43R contains two Cu^{2+}-binding sites: one with a higher Cu^{2+} affinity and lower pro-oxidant activity (higher-affinity site) and the other with a lower Cu^{2+} affinity and higher pro-oxidant activity (lower-affinity site). In both sites, His residues are bound to Cu^{2+} and involved in the pro-oxidant activity, as revealed by Raman spectroscopy and photooxidation. The number of His residues bound to Cu^{2+} in three different coordination types, HisNπ–Cu, HisNτ–Cu, and His^{-}–Cu_2, were evaluated from the intensities of the Raman bands. The observed numbers of HisNπ–Cu and HisNτ–Cu are 1.1 and 3.1, respectively, in the fully metalated state produced by the addition of 2.5 equiv of Cu^{2+} (Table 1). This observation suggests that the Cu^{2+}-binding sites contain one HisNπ–Cu and three HisNτ–Cu residues in total. In the presence of 1 equiv of Cu^{2+}, the number of Cu^{2+}-bound His decreases by 0.6 (from 1.1 to 0.5) for HisNπ–Cu and by 0.3 (from 3.1 to 2.8) for HisNτ–Cu (Table 1). Because the lower-affinity site is expected to lose more Cu^{2+} than the higher-affinity site upon the transition from the fully metalated to the half-filled state, the larger decrease of HisNπ–Cu (0.6) suggests that the unique HisNπ–Cu residue is located at the lower-affinity site. However, three HisNτ–Cu residues are likely to be located at the higher-affinity sites because the number of HisNτ–Cu would show a decrease of 0.6 or more if one or more HisNτ–Cu residues were also located at the lower-affinity site. In addition to the HisNπ–Cu and HisNτ–Cu coordination, His^{-}–Cu_2 was detected in the presence of 2.5 equiv of Cu^{2+}, although its number was only 0.3. It is possible that another His residue occasionally forms an imidazolate bridge between the higher- and lower-affinity sites besides being in the HisNπ–Cu, HisNτ–Cu, and/or Cu^{2+}-free forms.

On the basis of the considerations described above, we propose a tentative model for the Cu^{2+}-binding mode of denatured apo-H43R in Figure 8. In this model, the higher-affinity site is composed of four His residues, of which three are HisNτ–Cu. However, the lower-affinity site contains two His residues, of which one is HisNπ–Cu. The two binding sites share one His residue that occasionally forms an imidazolate bridge (His^{-}–Cu_2). The present model does not exclude the possibility of Cu^{2+} coordination of other amino acid residues, such as Asp and Glu, that were not detected by UV Raman spectroscopy.[51] Although the Cu^{2+}-binding mode in Figure 8 was derived from the Raman spectra recorded at room

dx.doi.org/10.1021/bi400370w | Biochemistry 2013, 52, 5184−5194

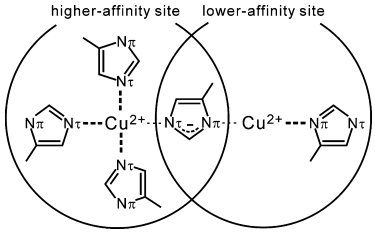

Figure 8. Tentative model for the Cu^{2+} binding mode of denatured apo-H43R. Up to two Cu^{2+} ions can bind to the protein monomer unit. One Cu^{2+}-binding site has higher affinity for Cu^{2+} than the other. In the higher-affinity site, three His residues are bound to Cu^{2+} via Nτ, whereas one His residue is bound to Cu^{2+} via Nπ in the lower-affinity site. Another His residue is shared by the two binding sites and occasionally forms an imidazolate bridge between the two Cu^{2+} ions besides being in the HisNπ−Cu, HisNτ−Cu, and/or Cu^{2+}-free forms. The positions of Nπ and Nτ of the bridging His residue are not certain. In addition to the His residues, the Cu^{2+} ions may be coordinated by other amino acid residues, such as Asp and Glu, that were not detected by UV Raman spectroscopy. The lower-affinity site exhibits higher pro-oxidant activity than the higher-affinity site.

temperature, the binding mode is thought to persist under physiological conditions because elevation of the temperature from 24 to 37 °C does not significantly affect the Cu^{2+} d−d absorption, which is a sensitive probe of Cu^{2+} coordination chemistry (Figure S2). It is strongly suggested that Cu^{2+}-bound denatured apo-H43R retains the pro-oxidant activity under physiological temperature.

Comparison of the Metal-Binding Mode between the Denatured and Native Forms. The present study has shown that His residues play a key role in the pro-oxidant Cu^{2+}-binding mode of denatured apo-H43R. H43R contains seven His residues per monomer unit. In the native holo form of H43R, one Cu^{2+} and one Zn^{2+} ion are bound to the protein.[52] The Cu^{2+}-binding site is composed of four His residues (His46, His48, His63, and His120), of which two are HisNτ−Cu, one is HisNπ−Cu, and the remaining one (His63) forms an imidazolate bridge between Cu^{2+} and Zn^{2+}. However, two His residues are bound to the metal ion through Nπ (like HisNπ−Cu) at the Zn^{2+}-binding site in addition to the His63 imidazolate bridge. The dominance of Nτ and Nπ coordination at the Cu^{2+}- and Zn^{2+}-binding sites, respectively, is analogous to that at the higher- and lower-affinity sites of denatured apo-H43R (Figure 8). However, the numbers of His residues in the three metal-coordination types differ between the denatured and native proteins, indicating a uniqueness of the Cu^{2+}-binding mode of denatured apo-H43R. The CD spectra have shown that apo-H43R unfolds from the β-barrel structure during the denaturation and locally refolds in the presence of Cu^{2+} (Figure 1). The denaturation process may destroy the structures of native metal-binding sites and even change the locations of His residues. The addition of Cu^{2+} is likely to induce rearrangement of His residues and to create new binding sites that exert pro-oxidant activity. Interestingly, the lower-affinity Cu^{2+}-binding site exhibits higher pro-oxidant activity than the higher-affinity Cu^{2+} binding site (Figure 3). Nonrigid coordination by His may be favorable for pro-oxidant activity at the Cu^{2+} catalytic center.

Relationship between the Cu^{2+}-Induced Pro-Oxidant Activity of Denatured Apo-H43R and ALS. The motor cortex and spinal cord of ALS patients exhibit increased levels of oxidative damage to proteins, lipids, and nucleic acids.[53] The concentration of reactive oxygen species as well as the degree of oxidative damage is also elevated in transgenic mice and cells expressing ALS-linked mutants of human SOD1.[54−59] Accordingly, oxidative stress is regarded as a key factor leading to the pathogenesis of ALS.[13−17] In this study, we have shown that a denatured form of an ALS-linked SOD1 mutant binds Cu^{2+} ions and gains pro-oxidant activity in the presence of H_2O_2. Once these pro-oxidant Cu^{2+} centers are formed, the cellular oxidative stress may be increased by ambient H_2O_2, whose in vivo concentration ranges from 10^{-2} to 10^{2} μM.[60]

The importance of Cu^{2+} in the pathogenesis of ALS has been demonstrated by the observation that a genetically decreased Cu^{2+} concentration in the spinal cord or the administration of a Cu^{2+} chelator delays the onset of the disease and extends survival in a transgenic mouse model of ALS.[61,62] Preliminary studies in our laboratory suggest that other ALS-linked mutants, A4V and G93A, in the apo state also undergo denaturation at 37 °C and exhibit pro-oxidant activity in the presence of Cu^{2+} and H_2O_2 similar to that of H43R. The binding of Cu^{2+} to denatured SOD1 protein may be a key step in the development of ALS, at least for patients carrying certain types of SOD1 mutants.

The native holo form of SOD1 is prepared by post-translational modifications of disulfide-reduced, metal-unbound (apo), immature SOD1. The Cu^{2+} ion is inserted into the Cu^{2+}-binding site of immature SOD1 by the copper chaperone for SOD1 (CCS).[63] This normal Cu-loading process may not apply to the H43R mutant because H43R in the apo state readily unfolds at physiological temperature, as shown in this study, and the unfolded protein structure would not be properly recognized by CCS.[64,65] Nevertheless, the unfolded apo protein is likely to bind Cu ions that are improperly released from CCS or supplied by CCS-independent pathways.[66] In actuality, SOD1 is abundant in motor neurons (1 to 2% of total proteins),[67] and ALS-linked mutations induce an increase in the affinity for Cu,[68] resulting in an accumulation of Cu in motor neurons expressing mutant SOD1, such as H43R.[69] Because the intracellular concentrations of SOD1 and Cu are comparable to those used in the present in vitro experiments,[70] the Cu^{2+}-binding mode of denatured apo-H43R revealed here may also apply in vivo. The Cu^{2+}-binding mode in Figure 8 is thus expected to be useful for elucidating the molecular mechanism of pro-oxidant activity of ALS-linked SOD1 mutants and their roles in the pathogenesis of ALS.

■ CONCLUSIONS

Denatured apo-H43R contains two Cu^{2+}-binding sites with higher and lower Cu^{2+} affinities. The higher-affinity site exhibits lower pro-oxidant activity and contains three His residues bound to Cu^{2+} via Nτ. However, the lower-affinity site has higher pro-oxidant activity and contains one His residue bound to Cu^{2+} via Nπ. An additional His residue occasionally forms an imidazolate bridge between the two Cu^{2+}-binding sites. The unfolding of apo-H43R during denaturation at 37 °C and subsequent local refolding upon binding of Cu^{2+} create the toxic Cu^{2+} catalytic sites. His residues are essential for both Cu^{2+} binding and pro-oxidant activity. The Cu^{2+}-binding mode of denatured apo-H43R may provide a clue for the structural mechanism underlying the cytotoxic role of denatured, mismetalated SOD1 mutants in the development of ALS.

dx.doi.org/10.1021/bi400370w | *Biochemistry* 2013, 52, 5184−5194

■ ASSOCIATED CONTENT

Supporting Information

UV (229 nm) Raman spectra of denatured apo-H43R/W32F and absorption spectra of denatured apo-H43R mixed with equimolar Cu^{2+}. This material is available free of charge via the Internet at http://pubs.acs.org.

■ AUTHOR INFORMATION

Corresponding Author

*Phone/Fax: +81-22-795-6855. E-mail: takeuchi@m.tohoku.ac.jp.

Notes

The authors declare no competing financial interest.

The authors declare no competing financial interest.

■ ABBREVIATIONS

ALS, amyotrophic lateral sclerosis; apo-H43R, apo form of H43R; BCA, bicinchoninic acid; CCS, copper chaperone for SOD1; CD, circular dichroism; DCF, 2′,7′-dichlorofluorescein; DCFH, 2′,7′-dichlorodihydrofluorescein; EDTA, ethylenediaminetetraacetic acid; H43R, His43Arg mutant of human SOD1; IMAC, immobilized metal-ion affinity chromatography; β-ME, β-mercaptoethanol; NTA, nitrilotriacetic acid; PAR, 4-(2-pyridylazo)resorcinol; RB, rose bengal; SOD1, Cu,Zn-superoxide dismutase

■ REFERENCES

(1) Rosen, D. R., Siddique, T., Patterson, D., Figlewicz, D. A., Sapp, P., Hentati, A., Donaldson, D., Goto, J., O'Regan, J. P., Deng, H. X., Rahmani, Z., Krizus, A., McKenna-Yasek, D., Cayabyab, A., Gaston, S., Tanzi, R., Halperin, J. J., Herzfeldt, B., Van den Berg, R., Hung, W.-Y., Bird, T., Deng, G., Mulder, D. W., Smith, C., Laing, N. G., Soriano, E., Pericak-Vance, M. A., Haines, J., Rouleau, G. A., Gusella, J., Horvitz, H. R., and Brown, R. H., Jr. (1993) Mutations in Cu/Zn superoxide dismutase gene are associated with familial amyotrophic lateral sclerosis. *Nature 362*, 59−62.

(2) Deng, H.-X., Hentati, A., Tainer, J. A., Iqbal, Z., Cayabyab, A., Hung, W.-Y., Getzoff, E. D., Hu, P., Herzfeldt, B., Roos, R. P., Warner, C., Deng, G., Soriano, E., Smyth, C., Parge, H. E., Ahmed, A., Roses, A. D., Hallewell, R. A., Pericak-Vance, M. A., and Siddique, T. (1993) Amyotrophic lateral sclerosis and structural defects in Cu,Zn superoxide dismutase. *Science 261*, 1047−1051.

(3) Cleveland, D. W., and Rothstein, J. D. (2001) From Charcot to Lou Gehrig: Deciphering selective motor neuron death in ALS. *Nat. Rev. Neurosci. 2*, 806−819.

(4) Valentine, J. S., Doucette, P. A., and Potter, S. Z. (2005) Copper-zinc superoxide dismutase and amyotrophic lateral sclerosis. *Annu. Rev. Biochem. 74*, 563−593.

(5) Rowland, L. P., and Shneider, N. A. (2001) Amyotrophic lateral sclerosis. *N. Engl. J. Med. 344*, 1688−1700.

(6) McCord, J. M., and Fridovich, I. (1969) Superoxide dismutase. An enzymic function for erythrocuprein (hemocuprein). *J. Biol. Chem. 244*, 6049−6055.

(7) Gurney, M. E., Pu, H., Chiu, A. Y., Dal Canto, M. C., Polchow, C. Y., Alexander, D. D., Caliendo, J., Hentati, A., Kwon, Y. W., Deng, H. X., Chen, W., Zhai, P., Sufit, R. L., and Siddique, T. (1994) Motor neuron degeneration in mice that express a human Cu,Zn superoxide dismutase mutation. *Science 264*, 1772−1775.

(8) Wong, P. C., Pardo, C. A., Borchelt, D. R., Lee, M. K., Copeland, N. G., Jenkins, N. A., Sisodia, S. S., Cleveland, D. W., and Price, D. L. (1995) An adverse property of a familial ALS-linked SOD1 mutation causes motor neuron disease characterized by vacuolar degeneration of mitochondria. *Neuron 14*, 1105−1116.

(9) Bruijn, L. I., Houseweart, M. K., Kato, S., Anderson, K. L., Anderson, S. D., Ohama, E., Reaume, A. G., Scott, R. W., and Cleveland, D. W. (1998) Aggregation and motor neuron toxicity of an ALS-linked SOD1 mutant independent from wild-type SOD1. *Science 281*, 1851−1854.

(10) Stathopulos, P. B., Rumfeldt, J. A., Scholz, G. A., Irani, R. A., Frey, H. E., Hallewell, R. A., Lepock, J. R., and Meiering, E. M. (2003) Cu/Zn superoxide dismutase mutants associated with amyotrophic lateral sclerosis show enhanced formation of aggregates in vitro. *Proc. Natl. Acad. Sci. U.S.A. 100*, 7021−7026.

(11) Furukawa, Y., and O'Halloran, T. V. (2005) Amyotrophic lateral sclerosis mutations have the greatest destabilizing effect on the apo- and reduced form of SOD1, leading to unfolding and oxidative aggregation. *J. Biol. Chem. 280*, 17266−17274.

(12) Deng, H. X., Shi, Y., Furukawa, Y., Zhai, H., Fu, R., Liu, E., Gorrie, G. H., Khan, M. S., Hung, W. Y., Bigio, E. H., Lukas, T., Dal Canto, M. C., O'Halloran, T. V., and Siddique, T. (2006) Conversion to the amyotrophic lateral sclerosis phenotype is associated with intermolecular linked insoluble aggregates of SOD1 in mitochondria. *Proc. Natl. Acad. Sci. U.S.A. 103*, 7142−7147.

(13) Wiedau-Pazos, M., Goto, J. J., Rabizadeh, S., Gralla, E. B., Roe, J. A., Lee, M. K., Valentine, J. S., and Bredesen, D. E. (1996) Altered reactivity of superoxide dismutase in familial amyotrophic lateral sclerosis. *Science 271*, 515−518.

(14) Yim, M. B., Kang, J. H., Yim, H. S., Kwak, H. S., Chock, P. B., and Stadtman, E. R. (1996) A gain-of-function of an amyotrophic lateral sclerosis-associated Cu,Zn-superoxide dismutase mutant: An enhancement of free radical formation due to a decrease in K_m for hydrogen peroxide. *Proc. Natl. Acad. Sci. U.S.A. 93*, 5709−5714.

(15) Ghadge, G. D., Lee, J. P., Bindokas, V. P., Jordan, J., Ma, L., Miller, R. J., and Roos, R. P. (1997) Mutant superoxide dismutase-1-linked familial amyotrophic lateral sclerosis: Molecular mechanisms of neuronal death and protection. *J. Neurosci. 17*, 8756−8766.

(16) Said Ahmed, M., Hung, W. Y., Zu, J. S., Hockberger, P., and Siddique, T. (2000) Increased reactive oxygen species in familial amyotrophic lateral sclerosis with mutations in SOD1. *J. Neurol. Sci. 176*, 88−94.

(17) Beretta, S., Sala, G., Mattavelli, L., Ceresa, C., Casciati, A., Ferri, A., Carrì, M. T., and Ferrarese, C. (2003) Mitochondrial dysfunction due to mutant copper/zinc superoxide dismutase associated with amyotrophic lateral sclerosis is reversed by N-acetylcysteine. *Neurobiol. Dis. 13*, 213−221.

(18) Strange, R. W., Antonyuk, S., Hough, M. A., Doucette, P. A., Rodriguez, J. A., Hart, P. J., Hayward, L. J., Valentine, J. S., and Hasnain, S. S. (2003) The structure of holo and metal-deficient wild-type human Cu, Zn superoxide dismutase and its relevance to familial amyotrophic lateral sclerosis. *J. Mol. Biol. 328*, 877−891.

(19) Arnesano, F., Banci, L., Bertini, I., Martinelli, M., Furukawa, Y., and O'Halloran, T. V. (2004) The unusually stable quaternary structure of human Cu,Zn-superoxide dismutase 1 is controlled by both metal occupancy and disulfide status. *J. Biol. Chem. 279*, 47998−48003.

(20) Rakhit, R., and Chakrabartty, A. (2006) Structure, folding, and misfolding of Cu,Zn superoxide dismutase in amyotrophic lateral sclerosis. *Biochim. Biophys. Acta 1762*, 1025−1037.

(21) Kitamura, F., Fujimaki, N., Okita, W., Hiramatsu, H., and Takeuchi, H. (2011) Structural instability and Cu-dependent pro-oxidant activity acquired by the apo form of mutant SOD1 associated with amyotrophic lateral sclerosis. *Biochemistry 50*, 4242−4250.

(22) Smith, P. K., Krohn, R. I., Hermanson, G. T., Mallia, A. K., Gartner, F. H., Provenzano, M. D., Fujimoto, E. K., Goeke, N. M., Olson, B. J., and Klenk, D. C. (1985) Measurement of protein using bicinchoninic acid. *Anal. Biochem. 150*, 76−85.

(23) Široki, M., Marić, Lj., and Herak, M. J. (1976) Study of complexes involved in the determination of copper using 4-(2-pyridylazo)resorcinol. *Z. Anal. Chem. 278*, 285−286.

(24) Crow, J. P., Sampson, J. B., Zhuang, Y., Thompson, J. A., and Beckman, J. S. (1997) Decreased zinc affinity of amyotrophic lateral sclerosis-associated superoxide dismutase mutants leads to enhanced catalysis of tyrosine nitration by peroxynitrite. *J. Neurochem. 69*, 1936−1944.

(25) Westhead, E. D. (1965) Photooxidation with rose bengal of a critical histidine residue in yeast enolase. *Biochemistry 4*, 2139−2144.
(26) Martinez-Carrion, M., Turano, C., Riva, F., and Fasella, P. (1967) Evidence of a critical histidine residue in soluble aspartic aminotransferase. *J. Biol. Chem. 242*, 1426−1430.
(27) Pedersen, A. O., Schonheyder, F., and Brodersen, R. (1977) Photooxidation of human serum albumin and its complex with bilirubin. *Eur. J. Biochem. 72*, 213−221.
(28) Blount, J. F., Fraser, K. A., Freeman, H. C., Szymanski, J. T., and Wang, C.-H. (1967) Crystallographic studies of metal-peptide complexes. IV. (Glycyl-L-histidinato)copper(II) sesquihydrate. *Acta Crystallogr. 22*, 396−405.
(29) Freeman, H. C., and Szymanski, J. T. (1967) Crystallographic studies of metal-peptide complexes. V. (β-Alanyl-L-histidinato)copper-(II) dihydrate. *Acta Crystallogr. 22*, 406−417.
(30) Sato, M., Ikeda, M., Fukuda, M., Ikeda, T., and Nakaya, J. (1987) Formation and scission of the imidazolate-bridge linkage in binuclear copper(II) complex with glycylglycine as a function of pH in aqueous solution. *Inorg. Chim. Acta 136*, 47−52.
(31) Markham, L. M., Mayne, L. C., Hudson, B. S., and Zgierski, M. Z. (1993) Resonance Raman studies of imidazole, imidazolium, and their derivatives: the effect of deuterium substitution. *J. Phys. Chem. 97*, 10319−10325.
(32) Miura, T., Satoh, T., Hori-i, A., and Takeuchi, H. (1998) Raman marker bands of metal coordination sites of histidine side chains in peptides and proteins. *J. Raman Spectrosc. 29*, 41−47.
(33) Hashimoto, S., Ono, K., and Takeuchi, H. (1998) UV resonance Raman scattering from metal-coordinating histidine residues in Cu,Zn-dismutase. *J. Raman Spectrosc. 29*, 969−975.
(34) Miura, T., Hori-i, A., Mototani, H., and Takeuchi, H. (1999) Raman spectroscopic study on the copper(II) binding mode of prion octapeptide and its pH dependence. *Biochemistry 38*, 11560−11569.
(35) Wang, D., Zhao, X., Vargek, M., and Spiro, T. G. (2000) Metal-bound histidine modes in UV resonance Raman spectra of Cu, Zn superoxide dismutase. *J. Am. Chem. Soc. 122*, 2193−2199.
(36) Takeuchi, H. (2003) Raman structural markers of tryptophan and histidine side chains in proteins. *Biopolymers 72*, 305−317.
(37) Toyama, A., Takahashi, Y., and Takeuchi, H. (2004) Catalytic and structural role of a metal-free histidine residue in bovine Cu-Zn superoxide dismutase. *Biochemistry 43*, 4670−4679.
(38) Takeuchi, H. (2011) UV Raman markers for structural analysis of aromatic side chains in proteins. *Anal. Sci. 27*, 1077−1086.
(39) Sundius, T. (1973) Computer fitting of Voigt profiles to Raman lines. *J. Raman Spectrosc. 1*, 471−488.
(40) Thompson, W. J. (1993) Numerous neat algorithms for the Voigt profile function. *Comput. Phys. 7*, 627−631.
(41) Brahms, S., and Brahms, J. (1980) Determination of protein secondary structure in solution by vacuum ultraviolet circular dichroism. *J. Mol. Biol. 138*, 149−178.
(42) Wardman, P. (2007) Fluorescent and luminescent probes for measurement of oxidative and nitrosative species in cells and tissues: Progress, pitfalls, and prospects. *Free Radical Biol. Med. 43*, 995−1022.
(43) Knepper, T. P. (2003) Synthetic chelating agents and compounds exhibiting complexing properties in the aquatic environment. *Trends Anal. Chem. 22*, 708−724.
(44) Asher, S. A., Ludwig, M., and Johnson, C. R. (1986) UV resonance Raman excitation profiles of the aromatic amino acids. *J. Am. Chem. Soc. 108*, 3186−3197.
(45) Fodor, S. P. A., Copeland, R. A., Grygon, C. A., and Spiro, T. G. (1989) Deep-ultraviolet Raman excitation profiles and vibronic scattering mechanisms of phenylalanine, tyrosine, and tryptophan. *J. Am. Chem. Soc. 111*, 5509−5518.
(46) Chi, Z., Chen, X. G., Holtz, J. S. W., and Asher, S. A. (1998) UV resonance Raman-selective amide vibrational enhancement: Quantitative methodology for determining protein secondary structure. *Biochemistry 37*, 2854−2864.
(47) Harada, I., and Takeuchi, H. (1986) Raman and ultraviolet resonance Raman spectra of proteins and related compounds, in *Spectroscopy of Biological Systems* (Clark, R. J. H., and Hester, R. E., Eds.) pp 113−175, Wiley, New York.
(48) Li, H., Wurrey, C. J., and Thomas, G. J., Jr. (1992) Cysteine conformation and sulfhydryl interactions in proteins and viruses. 2. Normal coordinate analysis of the cysteine side chain in model compounds. *J. Am. Chem. Soc. 114*, 7463−7469.
(49) Tasumi, M., Takahashi, S., Nakata, T., and Miyazawa, T. (1975) Infrared spectra and structures of copper(II) and zinc(II) complexes of glycylglycine in aqueous solution. *Bull. Chem. Soc. Jpn. 48*, 1595−1598.
(50) Fu, D., and Robyt, J. F. (1988) Essential histidine residues in dextransucrase: chemical modification by diethyl pyrocarbonate and dye photo-oxidation. *Carbohydr. Res. 183*, 97−109.
(51) Rubino, J. T., and Franz, K. J. (2012) Coordination chemistry of copper proteins: how nature handles a toxic cargo for essential function. *J. Inorg. Biochem. 107*, 129−143.
(52) DiDonato, M., Craig, L., Huff, M. E., Thayer, M. M., Cardoso, R. M., Kassmann, C. J., Lo, T. P., Bruns, C. K., Powers, E. T., Kelly, J. W., Getzoff, E. D., and Tainer, J. A. (2003) ALS mutants of human superoxide dismutase form fibrous aggregates via framework destabilization. *J. Mol. Biol. 332*, 601−615.
(53) Ferrante, R. J., Browne, S. E., Shinobu, L. A., Bowling, A. C., Baik, M. J., MacGarvey, U., Kowall, N. W., Brown, R. H., Jr., and Beal, M. F. (1997) Evidence of increased oxidative damage in both sporadic and familial amyotrophic lateral sclerosis. *J. Neurochem. 69*, 2064−2074.
(54) Zimmerman, M. C., Oberley, L. W., and Flanagan, S. W. (2007) Mutant SOD1-induced neuronal toxicity is mediated by increased mitochondrial superoxide levels. *J. Neurochem. 102*, 609−618.
(55) Liu, D., Wen, J., Liu, J., and Li, L. (1999) The roles of free radicals in amyotrophic lateral sclerosis: Reactive oxygen species and elevated oxidation of protein, DNA, and membrane phospholipids. *FASEB J. 13*, 2318−2328.
(56) Poon, H. F., Hensley, K., Thongboonkerd, V., Merchant, M. L., Lynn, B. C., Pierce, W. M., Klein, J. B., Calabrese, V., and Butterfield, D. A. (2005) Redox proteomics analysis of oxidatively modified proteins in G93A-SOD1 transgenic mice − a model of familial amyotrophic lateral sclerosis. *Free Radical Biol. Med. 39*, 453−462.
(57) Andrus, P. K., Fleck, T. J., Gurney, M. E., and Hall, E. D. (1998) Protein oxidative damage in a transgenic mouse model of familial amyotrophic lateral sclerosis. *J. Neurochem. 71*, 2041−2048.
(58) Liu, R., Althaus, J. S., Ellerbrock, B. R., Becker, D. A., and Gurney, M. E. (1998) Enhanced oxygen radical production in a transgenic mouse model of familial amyotrophic lateral sclerosis. *Ann. Neurol. 44*, 763−770.
(59) Warita, H., Hayashi, T., Murakami, T., Manabe, Y., and Abe, K. (2001) Oxidative damage to mitochondrial DNA in spinal motoneurons of transgenic ALS mice. *Brain Res. Mol. Brain Res. 89*, 147−152.
(60) Giorgio, M., Trinei, M., Migliaccio, E., and Pelicci, P. G. (2007) Hydrogen peroxide: a metabolic by-product or a common mediator of ageing signals? *Nat. Rev. Mol. Cell Biol. 8*, 722−728.
(61) Kiaei, M., Bush, A. I., Morrison, B. M., Morrison, J. H., Cherny, R. A., Volitakis, I., Beal, N. F., and Gordon, J. W. (2004) Genetically decreased spinal cord copper concentration prolongs life in a transgenic mouse model of amyotrophic lateral sclerosis. *J. Neurosci. 24*, 7945−7950.
(62) Hottinger, A. F., Fine, E. G., Gurney, M. E., Zurn, A. D., and Aebischer, P. (1997) The copper chelator d-penicillamine delays onset of disease and extends survival in a transgenic mouse model of familial amyotrophic lateral sclerosis. *Eur. J. Neurosci. 9*, 1548−1551.
(63) Furukawa, Y., and O' Halloran, T. V. (2006) Posttranslational modifications in Cu,Zn-superoxide dismutase and mutations associated with amyotrophic lateral sclerosis. *Antioxid. Redox Signaling 8*, 847−867.
(64) Schmidt, P. J., Kunst, C., and Culotta, V. C. (2000) Copper activation of superoxide dismutase 1 (SOD1) in vivo. *J. Biol. Chem. 275*, 33771−33776.
(65) Seetharaman, S. V., Prudencio, M., Karch, C., Holloway, S. P., Borchelt, D. R., and Hart, P. J. (2009) Immature copper-zinc

superoxide dismutase and familial amyotrophic lateral sclerosis. *Exp. Biol. Med. (Totowa, NJ, U.S.) 234*, 1140−1154.
(66) Carroll, M. C., Girouard, J. B., Ulloa, J. L., Subramaniam, J. R., Wong, P. C., Valentine, J. S., and Culotta, V. C. (2004) Mechanisms for activating Cu- and Zn-containing superoxide dismutase in the absence of the CCS Cu chaperone. *Proc. Natl. Acad. Sci. U.S.A. 101*, 5964−5969.
(67) Pardo, C. A., Xu, Z., Borchelt, D. R., Price, D. L., Sisodia, S. S., and Cleveland, D. W. (1995) Superoxide dismutase is an abundant component in cell bodies, dendrites, and axons of motor neurons and in a subset of other neurons. *Proc. Natl. Acad. Sci. U.S.A. 92*, 954−958.
(68) Watanabe, S., Nagano, S., Duce, J., Kiaei, M., Li, Q. X., Tucker, S. M., Tiwari, A., Brown, R. H., Jr., Beal, M. F., Hayward, L. J., Culotta, V. C., Yoshihara, S., Sakoda, S., and Bush, A. I. (2007) Increased affinity for copper mediated by cysteine 111 in forms of mutant superoxide dismutase 1 linked to amyotrophic lateral sclerosis. *Free Radical Biol. Med. 42*, 1534−1542.
(69) Tokuda, E., Okawa, E., and Ono, S. (2009) Dysregulation of intracellular copper trafficking pathway in a mouse model of mutant copper/zinc superoxide dismutase-linked familial amyotrophic lateral sclerosis. *J. Neurochem. 111*, 181−191.
(70) Rae, T. D., Schmidt, P. J., Pufahl, R. A, Culotta, V. C, and O'Halloran, T. V. (1999) Undetectable intracellular free copper: the requirement of a copper chaperone for superoxide dismutase. *Science 284*, 805−808.